World Journal of Advanced Research and Reviews
eISSN: 2581-9615 CODEN (USA): WJARAI
Cross Ref DOI: 10.30574/wjarr
Journal homepage: https://wjarr.com/

(RESEARCH ARTICLE)

Check for updates

Python-based seismic-to-well tie, horizon interpretation and structural mapping for reservoir characterization in the Niger Delta Basin

Onengiyeofori. A. Davies *, Opiriyabo I. Horsfall, Paddy A. Ngeri and Jiriwari Amonieah

Physics Department, Faculty of Science, Rivers State University, Port Harcourt, Rivers State, Nigeria.

World Journal of Advanced Research and Reviews, 2026, 30(02), 2277-2291

Publication history: Received on 12 April 2026; revised on 25 May 2026; accepted on 27 May 2026

Article DOI: https://doi.org/10.30574/wjarr.2026.30.2.1502

Abstract

This study presents a Python-based workflow for seismic-to-well tying, reservoir correlation, and structural mapping using well-log and 3D seismic data from the Kolo Creek Field in the Niger Delta Basin. The study aimed to evaluate the applicability of open-source scientific computing tools for seismic interpretation and reservoir characterization traditionally performed using proprietary software. Gamma ray, resistivity, sonic, and density logs were integrated with 3D seismic data for reservoir identification, synthetic seismogram generation, seismic-to-well tying, horizon interpretation, and structural mapping. Acoustic impedance and reflection coefficient series were computed from the sonic and density logs, after which synthetic seismograms were generated using a $25Hz$ zero-phase Ricker wavelet. The results revealed laterally continuous reservoir intervals with depths ranging from $11{,}598ft$ to $12{,}248ft$ across the study area. Seismic-to-well tying identified the reservoir top at approximately $978.87ms$ two-way travel time and produced a calibrated average interval velocity of approximately $24{,}016ft/s$ for depth conversion. The generated time and depth structure maps revealed a regional structural dip with localized structural closures that may represent favorable hydrocarbon trapping configurations. Comparison between the Python-derived depth structure map and a previously published Petrel-derived interpretation showed strong agreement in structural trends and contour geometry. The study demonstrates that Python-based workflows provide a reliable, reproducible, and cost-effective framework for seismic interpretation, structural mapping, and reservoir characterization within academic and research environments.

Keywords: Seismic-To-Well Tie; Reservoir Characterization; Structural Mapping; Niger Delta; Python Workflow

1. Introduction

Reservoir characterization remains an important aspect of hydrocarbon exploration and field development because it provides insight into subsurface structure, reservoir continuity, and potential trapping conditions within sedimentary basins [1, 2]. In seismic reservoir studies, one of the most widely applied approaches for linking geological information from wells with subsurface seismic reflections is seismic-to-well tying [3, 4]. Through this process, reflection events observed on seismic sections can be calibrated to lithologic boundaries and reservoir intervals identified from well logs, thereby improving confidence in horizon interpretation and structural mapping.

Synthetic seismogram generation forms a fundamental component of seismic-to-well tie analysis. Acoustic impedance contrasts derived from sonic and density logs are transformed into reflection coefficient series and convolved with a seismic wavelet to generate synthetic traces that approximate real seismic responses [5-7]. Matching the synthetic trace with seismic reflections at the well location establishes the relationship between subsurface geology and seismic travel time, which subsequently guides horizon interpretation and depth conversion [8].

* Corresponding author: Onengiyeofori. A. Davies

Most seismic interpretation workflows involving synthetic seismogram generation, horizon picking, structural mapping, and depth conversion are traditionally performed using proprietary geophysical software platforms. While these platforms are widely used within the petroleum industry, their high licensing and maintenance costs often limit accessibility in academic and research environments, particularly in developing countries [9]. This limitation affects practical training, computational experimentation, and workflow reproducibility within university-based geoscience programs [10, 11].

Recent developments in open-source scientific computing have increased the application of Python in geophysical data analysis and seismic interpretation [12-15]. Python provides a flexible computational environment supported by libraries for numerical analysis, seismic visualization, scientific plotting, and well-log processing. These tools have created opportunities for developing reproducible and low-cost interpretation workflows that can support both research and teaching applications.

The Niger Delta Basin presents a suitable environment for evaluating such workflows because of its structurally complex growth-fault systems and interbedded sand-shale sequences associated with hydrocarbon accumulation [16-18]. Reservoir distribution within the basin is commonly controlled by rollover structures, fault-assisted closures, and stratigraphic variability, making seismic calibration and structural mapping important components of reservoir evaluation.

Although several studies have applied seismic-to-well tying and structural interpretation within the Niger Delta Basin [19-21], fewer studies have demonstrated integrated Python-based workflows that combine well-log correlation, synthetic seismogram generation, horizon interpretation, structural mapping, and depth conversion within a unified open-source framework [22]. This study therefore presents a Python-based workflow for seismic-to-well tying, horizon interpretation, and structural mapping using well-log and 3D seismic data from the Kolo Creek Field in the Niger Delta Basin. The study further evaluates the capability of open-source scientific computing tools to produce structurally reliable reservoir interpretations comparable to those generated using conventional commercial interpretation platforms.

1.1. Study Area and Geological Setting of the Study Area

The study was carried out using seismic and well-log data obtained from the Kolo Creek Field located within the onshore Niger Delta Basin, southern Nigeria. The Niger Delta is one of the most prolific hydrocarbon provinces in the world and has remained a major focus of petroleum exploration due to its large sedimentary thickness, favorable structural setting, and extensive hydrocarbon reserves [17, 18]. The basin occupies the Gulf of Guinea continental margin and developed during the separation of the African and South American plates in the Late Jurassic to Early Cretaceous [23].

Sedimentation within the Niger Delta occurred under a prograding deltaic system that resulted in the deposition of thick sequences of sands and shales [23]. The basin is generally subdivided into three major lithostratigraphic units: the Akata, Agbada, and Benin Formations [17, 18, 24]. The Akata Formation forms the basal marine shale unit and is widely regarded as the principal hydrocarbon source rock within the basin [25]. Overlying the Akata Formation is the Agbada Formation, which consists of alternating sandstone and shale sequences deposited in paralic environments [17]. The Agbada Formation contains most of the economically productive reservoirs in the Niger Delta [18]. The upper Benin Formation is predominantly composed of continental sands with minor shale intercalations and constitutes the freshwater-bearing section of the basin [24].

The Kolo Creek Field is characterized by typical Niger Delta structural features, including growth faults, rollover anticlines, and fault-assisted closures formed as a result of deformation that occurred during sediment deposition associated with rapid sediment loading [16, 26]. These structural elements play a significant role in hydrocarbon migration and trapping within the field [16]. Reservoir units in the area are commonly composed of stacked sandstone bodies interbedded with shale layers deposited under fluvio-deltaic conditions [18].

Several exploration and development activities carried out within the Kolo Creek Field have resulted in the acquisition of extensive well-log and 3D seismic datasets. The availability of these datasets makes the field suitable for seismic-to-well tie studies, structural interpretation, and reservoir characterization. In addition, the structural complexity and reservoir distribution within the field provide a suitable framework for evaluating the applicability of Python-based computational workflows in seismic interpretation and subsurface mapping.

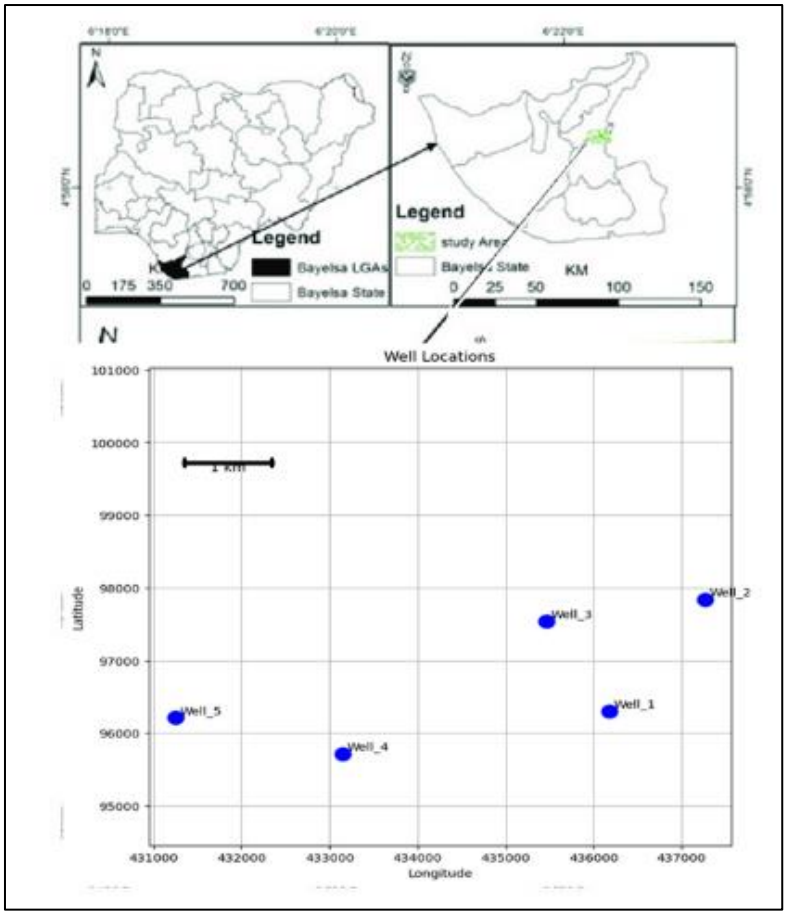

Figure 1 Location of the Study Area [27]

2. Material and methods

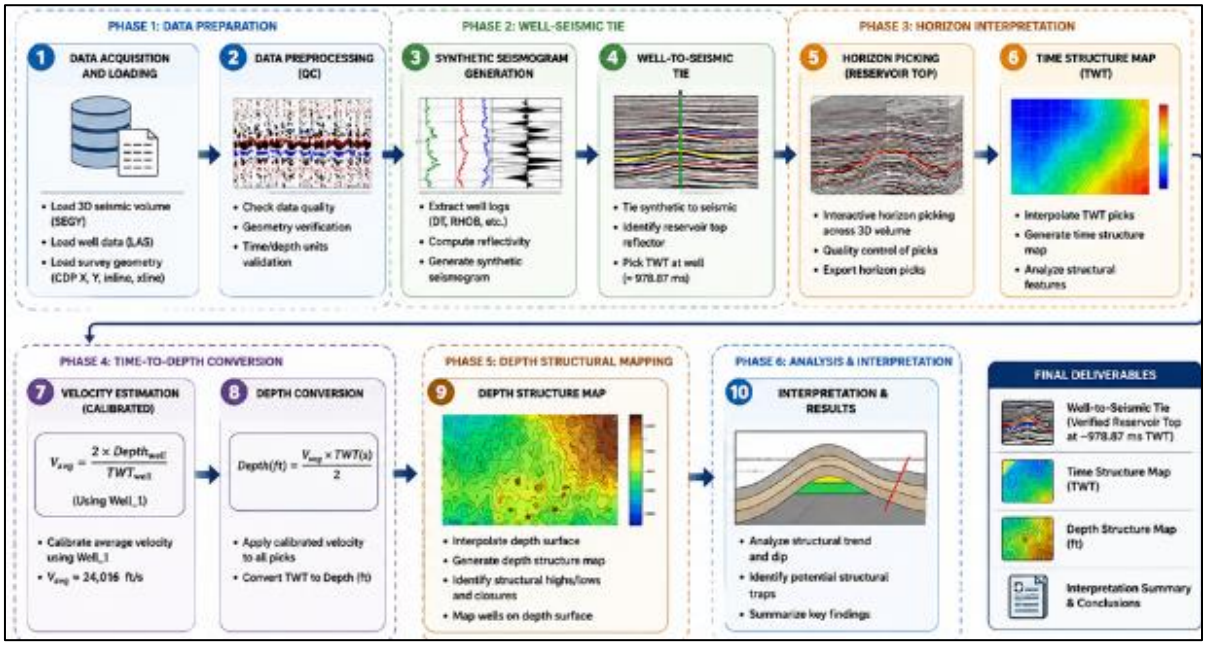

Figure 2 Research Workflow

2.1. Materials

The study utilized 3D post-stack seismic data (consisting of 849 inlines, 441 crosslines, and 1501-time samples recorded at a sampling interval of 4ms) and well-log data obtained from a reservoir interval within the Niger Delta Basin. The available well logs included gamma ray, resistivity, sonic, and density logs. The seismic data were stored in SEG-Y format, while the well logs were provided in LAS format. Python libraries such as NumPy, Pandas, Matplotlib, Plotly, SciPy, Segyio, Lasio and IPython Display were used for numerical computation and data management.

2.2. Method

The method employed in this research work is summarized in the workflow in figure 2.

2.2.1. Well Log Correlation

Reservoir intervals were identified and correlated across the available wells using gamma ray and resistivity logs. The gamma ray log was primarily used for lithologic discrimination because shale intervals generally exhibit higher gamma ray responses compared to cleaner sandstone units. Resistivity logs were subsequently used to identify intervals with relatively higher resistivity values that may indicate hydrocarbon-bearing sands.

The correlation process involved matching corresponding reservoir tops and bases across the wells based on similarities in log character and stratigraphic continuity. Correlated intervals were interpreted as laterally continuous reservoir units within the field. Well-log visualization and correlation panels were generated using Matplotlib.

2.2.2. Acoustic Impedance and Reflection Coefficient Estimation

Acoustic impedance (AI) was estimated from the sonic and density logs. According to Kamel and Mabrouk [28], acoustic impedance represents the resistance of a formation to seismic wave propagation and is expressed as:

$$AI = \rho v \qquad (1)$$

Where ρ is density and v is compressional velocity. The compressional velocity was estimated for the sonic log using the relationship in equation 2.

$$v = \frac{10^6}{\Delta t} \qquad (2)$$

Where Δt is the sonic transit time in microseconds per foot ($\mu s/ft$).

Changes in acoustic impedance across geological boundaries produce seismic reflections. Reflection coefficients (R) were therefore computed from adjacent impedance contrasts using equation 3.

$$R = \frac{A_i - A_{i-1}}{A_i + A_{i-1}} \qquad (3)$$

Where A_i and A_{i-1} are acoustic impedances of adjacent layers.

The reflection coefficient series provided a representation of the subsurface reflectivity structure required for synthetic seismic generation.

2.2.3. Synthetic Seismogram Generation

Synthetic seismograms were generated by convolving the reflection coefficient series with a seismic wavelet. The convolutional model assumes that a seismic trace can be represented as the convolution of the earth's reflectivity with a propagating seismic wavelet:

$$S(t) = W(t) \times R(t) \qquad (4)$$

Where $S(t)$ represents the synthetic seismic trace, $W(t)$ represents the seismic wavelet and $R(t)$ represents the reflectivity series.

A $25Hz$ zero-phase Ricker wavelet was adopted for this study. The choice of a zero-phase wavelet was considered appropriate because reservoir units within the Niger Delta are commonly interpreted using seismic data with dominant

frequencies within this range, providing an effective balance between vertical resolution and reflector continuity in sand-shale sequences. The Ricker wavelet is mathematically expressed according to Yilmaz [29] as seen in equation 5:

$$W(t) = (1 - 2\pi^2 f^2 t^2) e^{-\pi^2 f^2 t^2} \quad (5)$$

Where f is the dominant frequency and t is time.

Wavelet generation and convolution operations were implemented using NumPy and SciPy.

2.2.4. Time-Depth Relationship and Well Tie

The sonic log was used to establish the relationship between reservoir depth and seismic travel time. Since seismic reflections are recorded in two-way travel time (TWT), conversion between depth and time was necessary for seismic-to-well tying. Travel time was estimated through cumulative integration of interval transit times using equation 6.

$$TWT = 2 \int \frac{dz}{v(z)} \quad (6)$$

Where dz represents depthe increments and $v(z)$ represents interval velocity.

The generated synthetic seismogram was matched with the seismic trace nearest to the well position in order to identify the reflector corresponding to the reservoir interval. The well tie established a direct relationship between geological boundaries observed in the well logs and reflection events observed on the seismic section.

Based on the calibrated well tie, the average interval velocity (v_{avg}) was estimated using equation 7.

$$v_{avg} = \frac{2D}{TWT} \quad (7)$$

Where D is the reservoir depth.

2.2.5. Horizon Interpretation

Reservoir horizons were interpreted on inline and crossline seismic sections extracted from the 3D seismic volume. Interactive seismic visualization and horizon picking were performed using Plotly within the Python environment.

Manual interpretation was adopted because portions of the reservoir reflector exhibited variations in continuity and amplitude character. Manual picking allowed improved geological control during reflector tracking and reduced the likelihood of automated mispicks across structurally complex areas.

The interpreted picks were automatically stored and updated within a Pandas dataframe and exported into CSV format for subsequent structural mapping. Horizon tracking was guided by reflector continuity, amplitude consistency, and calibration from the seismic-to-well tie.

2.2.6. Structural Mapping

The interpreted horizon picks were used to generate time and depth structure maps. Spatial interpolation of the picks was performed using linear interpolation implemented through the SciPy library. Linear interpolation was preferred because it minimized artificial oscillations and unrealistic closures that may arise from higher-order interpolation methods according to Lemaire et. al. [30].

True seismic survey coordinates extracted from the SEG-Y headers (CDP_X and CDP_Y) were used instead of inline-crossline indices in order to preserve the actual geometry of the seismic survey. This approach produced geographically referenced structural maps that more accurately represented the spatial distribution of the reservoir surface.

Gaussian smoothing was subsequently applied to reduce localized picking noise and improve contour continuity across the mapped surface. Contour generation and map visualization were carried out using Matplotlib.

2.2.7. Depth Conversion

Depth conversion of the interpreted horizon was carried out using the calibrated average velocity model derived from the seismic-to-well tie. The conversion from time to depth was achieved using equation 8.

$$Depth = \frac{v_{avg} \times TWT}{2} \qquad (8)$$

The calibrated velocity approach was adopted because it preserved the structural geometry observed on the time map while producing geologically consistent depth contours across the study area. The final depth structure map was subsequently generated through interpolation and contouring of the converted depth values.

To evaluate the reliability of the developed Python-based workflow, the interpreted horizon was further compared with a previously published Petrel-derived depth structure map by Davies *et al* [31], generated from the same seismic and well-log datasets. The published Petrel interpretation served as a reference model for assessing the structural consistency of the Python-generated results. Comparative analysis between both interpretations was carried out based on contour geometry, regional dip orientation, and the spatial distribution of structural highs and lows across the reservoir interval.

3. Results

The results obtained from the integration of well-log and 3D seismic data within the Python-based interpretation workflow developed for the Kolo Creek Field are presented below. The results include well-log correlation, synthetic seismogram generation, seismic-to-well tie analysis, horizon interpretation, time structure mapping, and depth structure mapping of the identified reservoir interval.

The interpreted reservoir unit was identified and correlated across the available wells using gamma ray and resistivity logs, after which synthetic seismograms were generated from the sonic and density logs for seismic calibration. The seismic-to-well tie established a relationship between the reservoir interval and its corresponding seismic reflection event, thereby improving confidence in horizon identification and structural interpretation.

Interactive horizon picking was subsequently carried out on inline and crossline seismic sections, and the interpreted picks were used to generate time and depth structure maps of the reservoir top. The resulting structural maps were analysed to evaluate the geometry, continuity, and structural configuration of the reservoir within the study area.

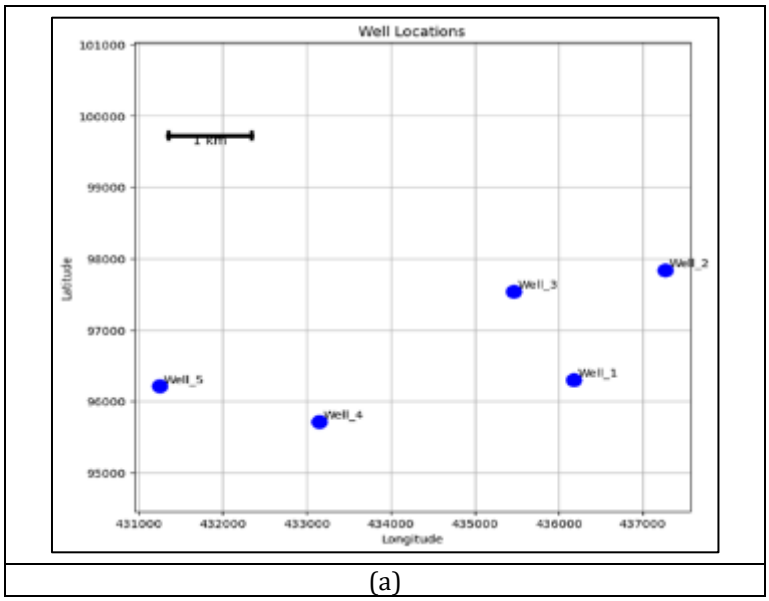

(a)

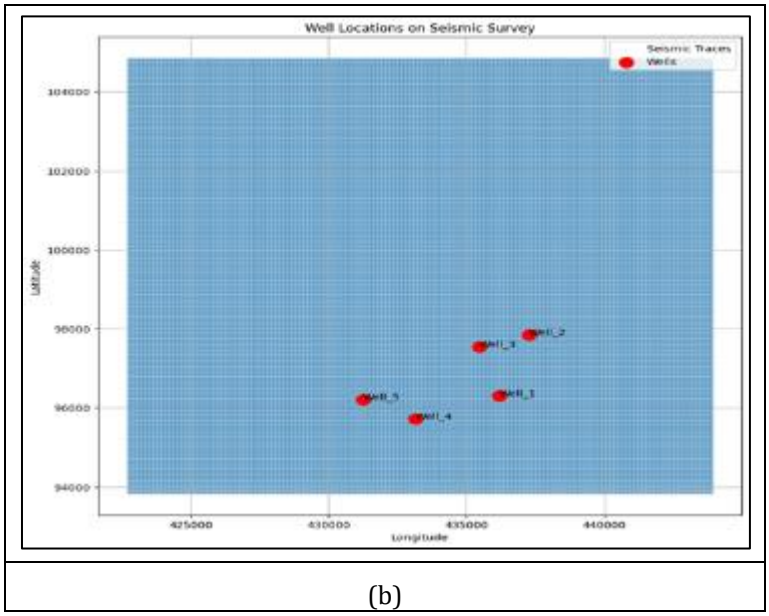

(b)

Figure 3 (a) Well locations in the study area (b) Well Location within the seismic geometry

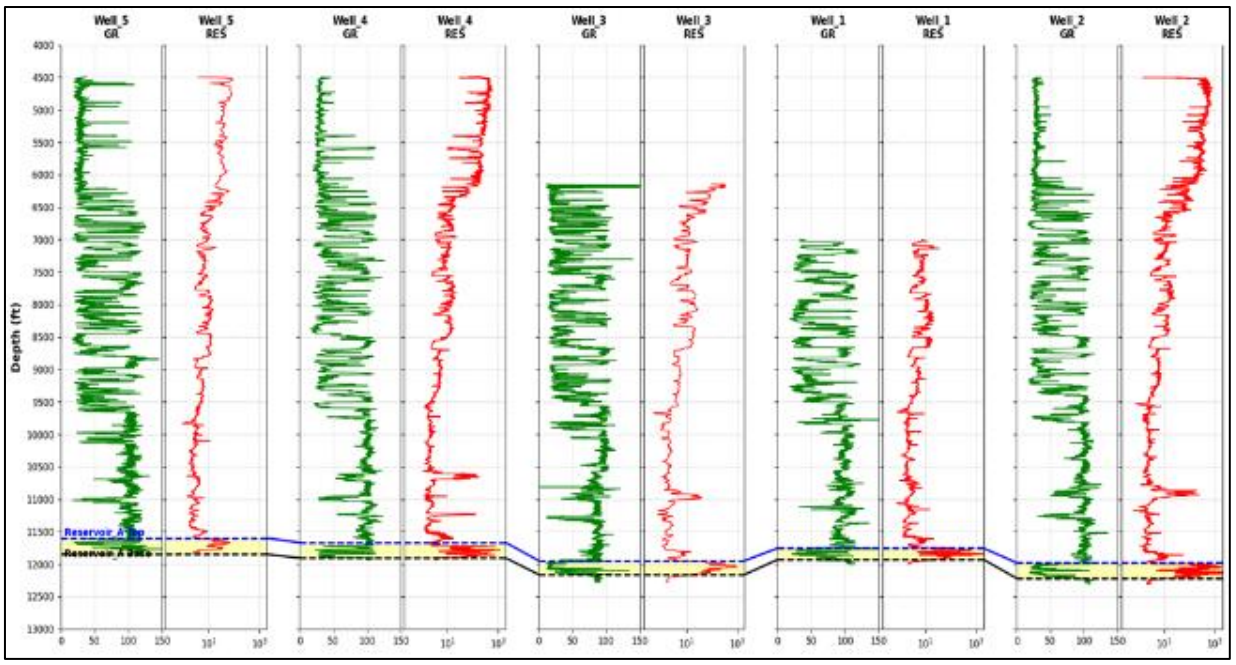

Figure 4 Correlated reservoir intervals

Table 1 Corelated reservoir intervals

Well	Reservoir Interval (ft)	Reservoir Thickness (ft)
Well-5	11598-11827	229
Well-4	11693-11925	232
Well-3	11949-12219	270
Well-1	11756-11942	186
Well-2	11962-12248	286

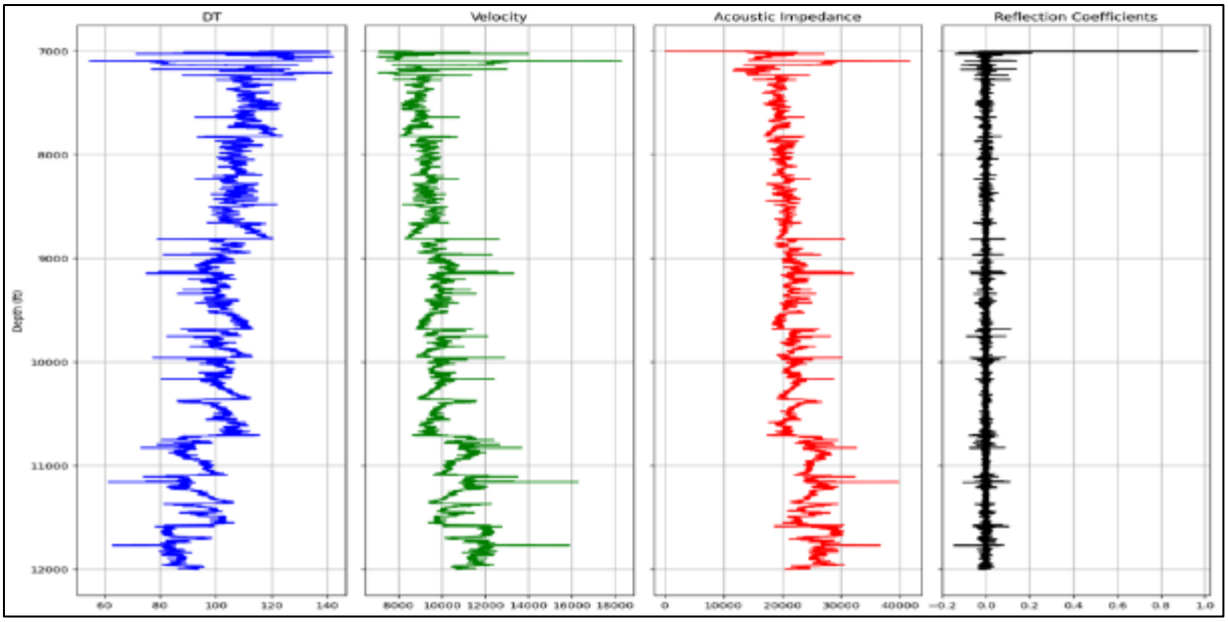

Figure 5 Traces of acoustic impedance and reflection coefficients

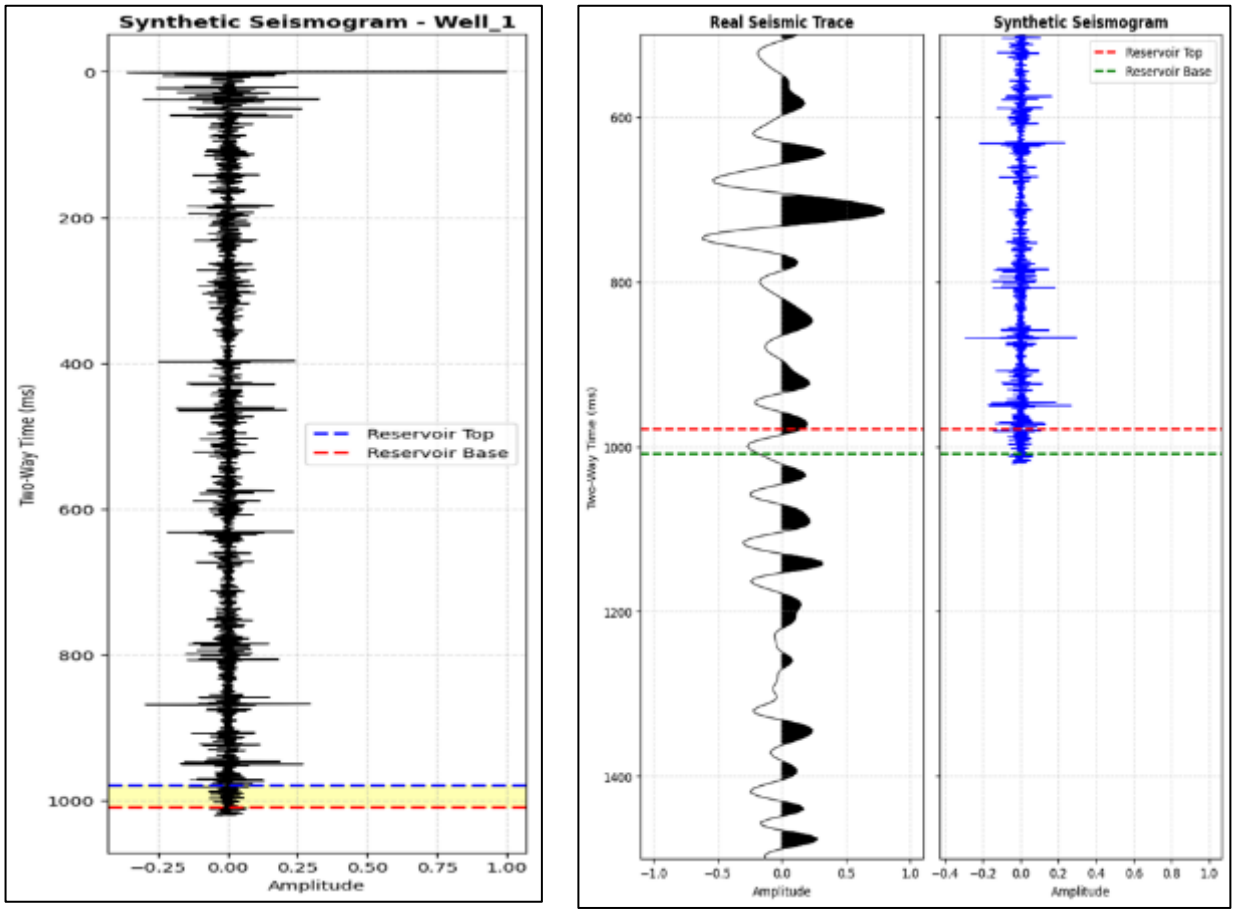

(a) (b)

Figure 6 (a) Correlated horizon on the synthetic seismogram (b) Synthetic seismogram tied to a real seismic trace

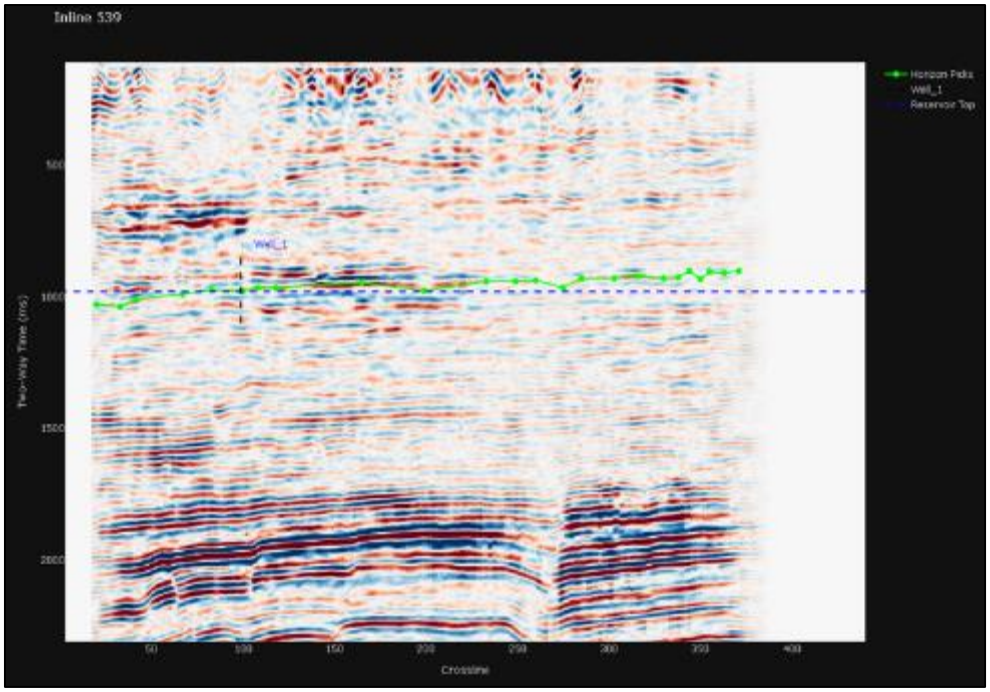

Figure 7 Interpreted horizon (green line) on inline 539 at the well location (black vertical line) guided by the correlated horizon (blue horizontal line)

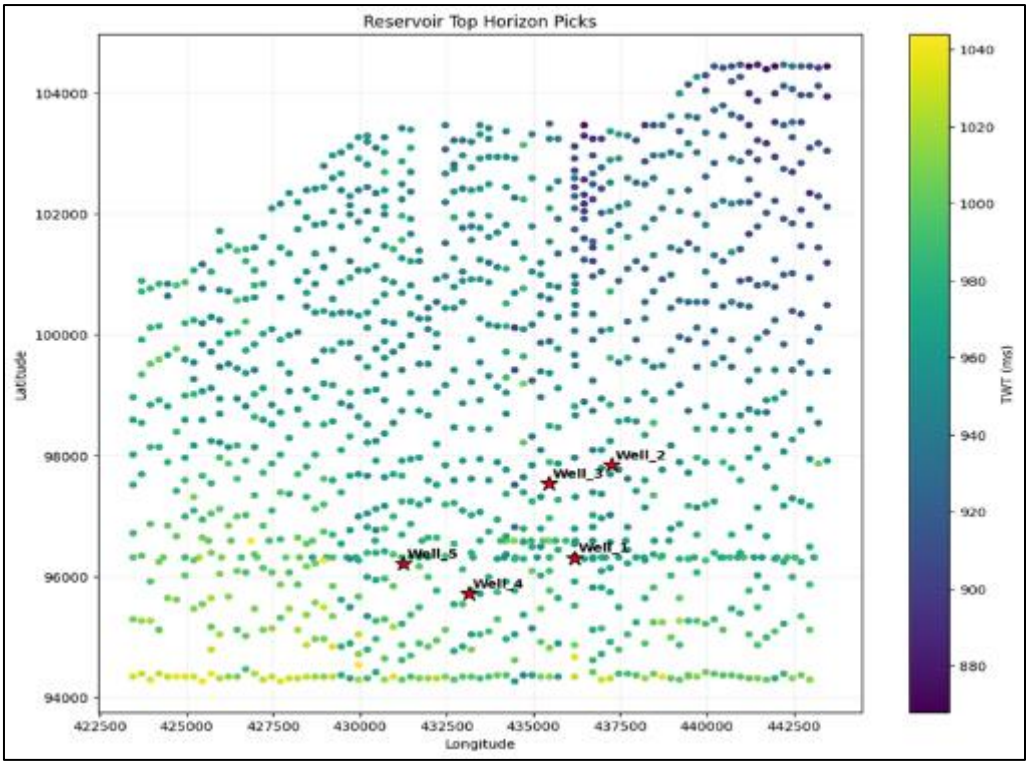

Figure 8 Picked horizons on the seismic section with well locations

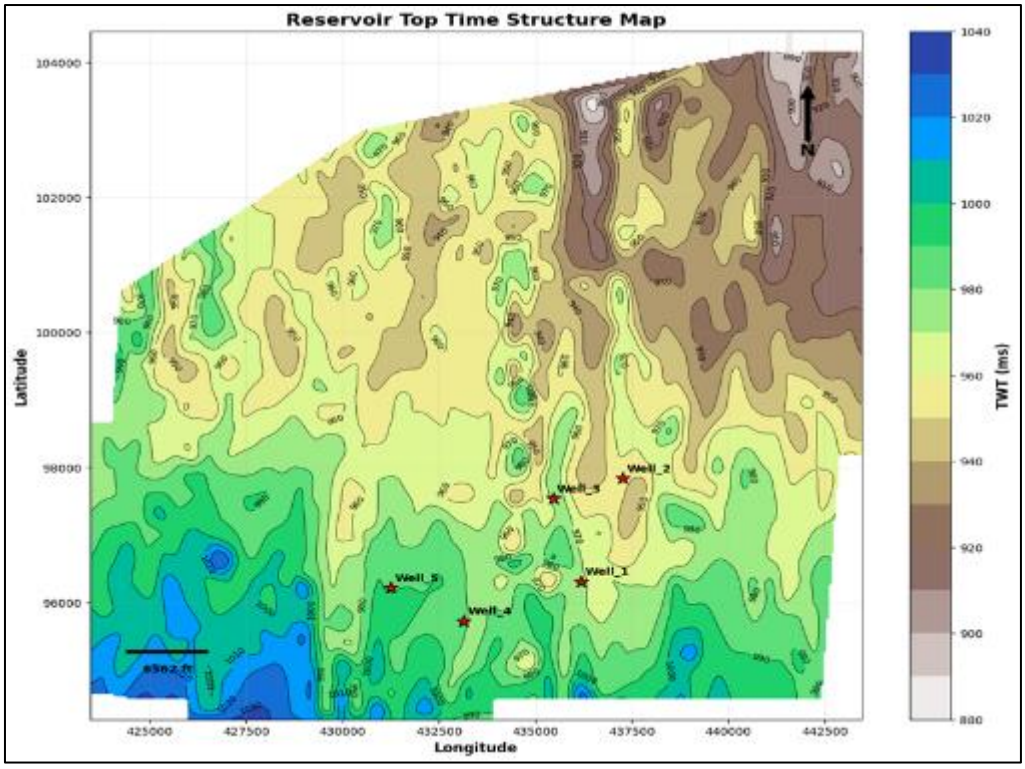

Figure 9 Time structural map

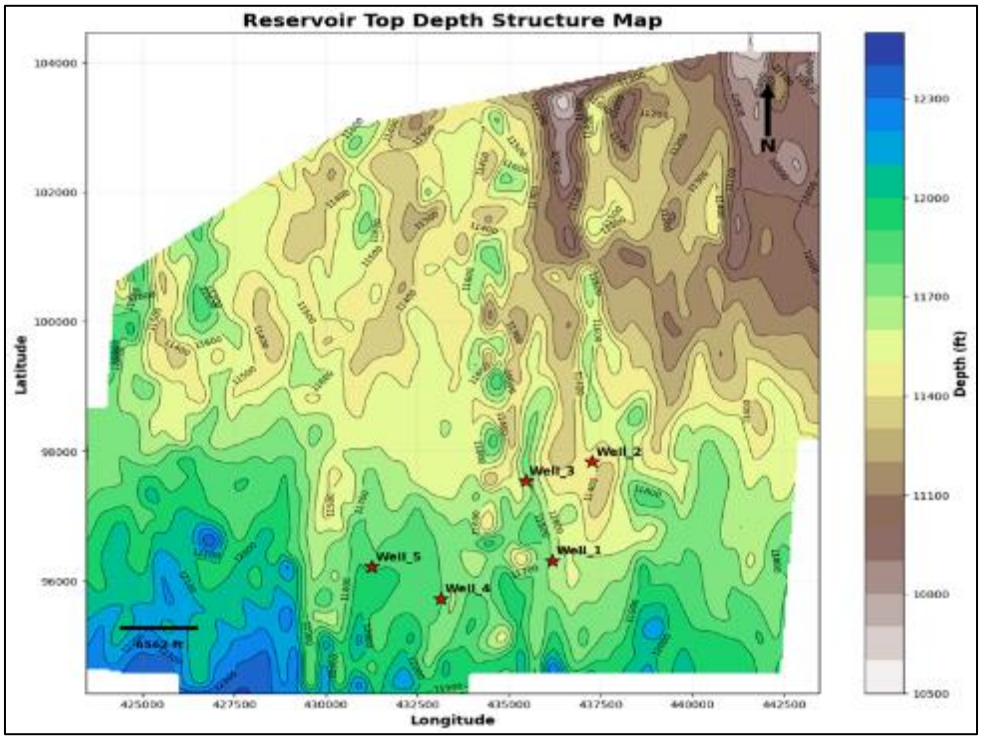

Figure 10 Depth structural map

Figure 11 presents the previously published Petrel-derived depth structure map of the reservoir interval interpreted from the same seismic dataset. The map provides a reference for evaluating the structural trends and contour patterns

obtained from the Python-based interpretation workflow. Similarities observed between both interpretations were subsequently used to assess the reliability of the generated depth structure within the study area.

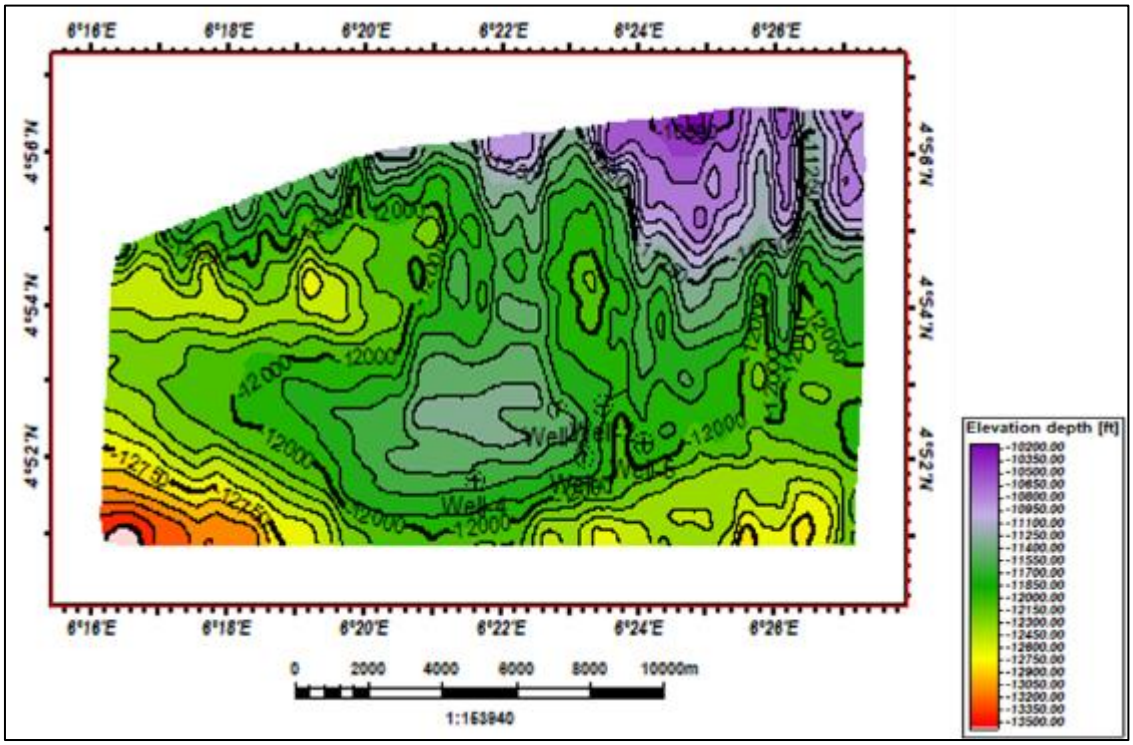

Figure 11 Petrel-derived depth structural map with the same dataset [31]

4. Discussion

The distribution of the wells within the seismic survey geometry shown in Figure 3 provided adequate spatial control for reservoir correlation and seismic calibration across the study area. The positioning of the wells across structurally different portions of the field improved confidence in the continuity of the interpreted reservoir interval and reduced uncertainty during horizon tracking and structural mapping.

The correlated reservoir intervals presented in Figure 4 and Table 1 exhibit relatively consistent log character across the wells, suggesting lateral continuity of the mapped sandstone unit within the field. The intervals are characterized by comparatively lower gamma ray responses and elevated resistivity values, which are consistent with sandstone reservoirs within the Agbada Formation of the Niger Delta Basin [32, 33]. Variations in reservoir thickness observed between the wells likely reflect localized depositional and structural influences associated with deltaic sedimentation and synsedimentary deformation within the basin [34]. The relatively thicker reservoir intervals encountered in Well-2 and Well-3 may indicate localized sand accumulation or structural preservation within those portions of the field [35].

The acoustic impedance and reflection coefficient traces shown in Figure 5 reveal distinct impedance contrasts across the reservoir interval, confirming the presence of acoustic boundaries capable of generating identifiable seismic reflections [36]. These impedance variations formed the basis for synthetic seismogram generation and seismic-to-well tying. The reasonable correspondence observed between the synthetic trace and the real seismic response in Figure 6 indicates that the generated synthetic seismogram adequately reproduced the seismic character of the reservoir interval. The adoption of a 25 Hz zero-phase Ricker wavelet contributed to improved reflector alignment because the symmetric wavelet response positioned reflection peaks and troughs directly over impedance boundaries. The identified reflector at approximately 978.87ms therefore provided the calibration required for subsequent horizon interpretation and structural mapping.

The interpreted horizon displayed in Figure 7 exhibits relatively continuous reflector character across the seismic section, suggesting lateral persistence of the mapped reservoir surface. The spatial distribution of the horizon picks shown in Figure 8 further indicates that the interpreted reflector was tracked consistently across the seismic volume. Although localized amplitude variations and reflector discontinuities were observed in some portions of the seismic

section, manual interpretation allowed improved geological control during reflector tracking, particularly within structurally disturbed regions where automated picking methods may produce unstable interpretations.

The time structure map presented in Figure 9 reveals a regional structural dip in which the reservoir generally deepens toward the northeastern portion of the field and becomes relatively shallower toward the southwest. This structural configuration is consistent with the growth-fault-controlled depositional architecture commonly associated with the Niger Delta Basin [37, 38]. The localized contour closures and structural undulations observed within the mapped surface may represent potential hydrocarbon trapping configurations associated with rollover deformation and fault-assisted structural development [18, 39]. These closures may also indicate areas of localized sediment accommodation and differential compaction within the reservoir interval [40].

Depth conversion of the interpreted horizon was carried out using the calibrated average depth-conversion velocity derived from the seismic-to-well tie relationship shown in equation 8. Using the tied reservoir depth from Well-1 and the corresponding seismic travel time, an average depth-conversion velocity of approximately 24,016 ft/s was derived and applied across the mapped interval. The estimated velocity is consistent with increasing sediment compaction and consolidation commonly associated with deeper Agbada Formation reservoirs within the Niger Delta Basin [41, 42]. Although the adopted velocity model represents a simplified average approximation, the resulting depth conversion preserved the overall structural geometry observed on the time map and produced geologically consistent depth contours across the study area.

The depth structure map shown in Figure 10 maintains the same general structural style observed on the time structure map, indicating that the applied velocity model introduced minimal structural distortion during depth conversion. The progressive deepening of the reservoir toward the northeastern section of the field may reflect increasing sediment loading and structural subsidence within that portion of the basin according to Wei *et. al.* [43]. In contrast, the relatively shallower southwestern region may represent structurally elevated portions of the reservoir that could favour hydrocarbon retention where adequate sealing conditions exist Abrams [44].

The comparison between the Python-derived depth structure map and the previously published Petrel-derived interpretation presented in Figure 11 demonstrates strong agreement in regional structural trends, contour orientation, and the spatial distribution of structural highs and lows across the reservoir interval. Both interpretations preserve the same general structural framework, particularly within the central and northeastern portions of the field where localized closures and contour deflections are evident. Minor differences between the maps are mainly associated with contour smoothness, local interpolation behaviour, and edge effects related to sparse horizon control near the survey boundaries. The smoother contour transitions observed in the Python-derived map are largely attributed to the application of Gaussian smoothing and interpolation within the Python workflow. Despite these differences, the overall correspondence between both interpretations indicates that the open-source workflow successfully reproduced the major structural characteristics of the reservoir interval. This agreement demonstrates the reliability of the Python-based approach for seismic interpretation, structural mapping, and reservoir characterization within the study area.

5. Conclusion

This study demonstrated the successful integration of well-log and 3D seismic data within a Python-based workflow for seismic-to-well tying, horizon interpretation, and structural mapping in the Kolo Creek Field of the Niger Delta Basin. The workflow enabled reliable reservoir correlation and produced structurally consistent time and depth maps that revealed a regional structural dip with localized closures associated with the fault-controlled depositional style of the Niger Delta Basin. The close agreement observed between the Python-derived depth structure map and the previously published Petrel-derived interpretation indicates that the developed workflow was capable of reproducing the major structural features of the reservoir interval with good reliability. This agreement further highlights the effectiveness of the adopted seismic calibration, horizon interpretation, and depth conversion procedures implemented within the open-source computational environment. Beyond the structural interpretation itself, the study demonstrates the growing potential of open-source scientific computing tools in applied geophysics. The integration of Python libraries for seismic visualization, well-log analysis, numerical computation, and structural mapping provided a flexible and reproducible framework for reservoir characterization without dependence on expensive proprietary software. The workflow developed in this study therefore offers practical value for academic research, geoscience training, and computational geophysics applications, particularly within environments where access to commercial interpretation platforms may be limited.

Compliance with ethical standards

Disclosure of conflict of interest

The authors declare that there are no conflicts of interest.

References

[1] Omoboriowo, A., et al., Reservoir characterization of Konga Field, Onshore Niger Delta, Southern Nigeria. International Journal of Emerging Technology, 2012. 3: p. 19-30.

[2] Digbani, T., et al., Integration of Core-Derived Facies Analysis And Well-Log Petrophysical Evaluation For Reservoir Characterization in the GABO Field, Onshore Niger Delta Basin. Journal of Applied Geology and Geophysics. 14(2): p. 30-39.

[3] Qin, N. and L.-Y. Fu, Reliability measurement of joint seismic inversion based on seismic-to-well correlation. Exploration Geophysics, 2013. 44(2): p. 87-103.

[4] Martínez, G.C., et al., Well-to-seismic tie, in Applied Techniques to Integrated Oil and Gas Reservoir Characterization. 2021, Elsevier. p. 249-271.

[5] Sheriff, R.E. and L.P. Geldart, Exploration seismology. 1995: Cambridge university press.

[6] Ning, L., et al., Development and prospect of acoustic reflection imaging logging processing and interpretation method. Petroleum Exploration and Development, 2024. 51(4): p. 839-851.

[7] de Macedo, I.A. and J.J.S. de Figueiredo, On the seismic wavelet estimative and reflectivity recovering based on linear inversion: Well-to-seismic tie on a real data set from Viking Graben, North Sea. Geophysics, 2020. 85(5): p. D157-D165.

[8] White, R. and R. Simm, Tutorial: Good practice in well ties. First Break, 2003. 21(10).

[9] Hall, B., Facies classification using machine learning. The Leading Edge, 2016. 35(10): p. 906-909.

[10] Ince, D.C., L. Hatton, and J. Graham-Cumming, The case for open computer programs. 2012. 482(7386): p. 485-488.

[11] Cohen-Boulakia, S., et al., Scientific workflows for computational reproducibility in the life sciences: Status, challenges and opportunities. Future Generation Computer Systems, 2017. 75: p. 284-298.

[12] Millman, K.J. and M. Aivazis, Python for Scientists and Engineers. Computing in Science and Engineering, 2011. 13(2): p. 9-12.

[13] Rücker, C., T. Günther, and F.M. Wagner, pyGIMLi: An open-source library for modelling and inversion in geophysics. Computers and Geosciences, 2017. 109: p. 106-123.

[14] Lemenkova, P., Processing oceanographic data by Python libraries NumPy, SciPy and Pandas. Aquatic Research, 2019. 2(2): p. 73-91.

[15] Uieda, L., et al. Harmonica and Boule: Modern Python tools for geophysical gravimetry. in EGU General Assembly Conference Abstracts. 2021.

[16] Weber, K. Petroleum geology of the Niger Delta. in Tokyo 9th World Petroleum Congress Proceedings, 1975. 1975.

[17] Short, K. and A. Stauble, Outline of geology of Niger Delta. AAPG bulletin, 1967. 51(5): p. 761-779.

[18] Doust, H., Petroleum geology of the Niger Delta. Geological Society, London, Special Publications, 1990. 50(1): p. 365-365.

[19] Davies, D.H., O.A. Davies, and O.I. Horsfall, Determination of Geomechanical Properties of a typical Niger Delta Reservoir Rock Using Geophysical Well Logs. Asian Journal of Applied science Technology, 2019. 3(1): p. 222-233.

[20] Salami, R. and A.O. Adepetun, Enhanced Reservoir Characterization of Phem Field, Offshore Niger Delta: Integration of Seismic Attributes and Reservoir Property Modeling. GeoScience Engineering, 2025. 71(2).

[21] Inichinbia, S. and A. Ahmed, Seismic-to-well tie of a field of the Nigerian Delta. Scientia Africana, 2020. 19(3): p. 125-138.

[22] Ita, E., D. Appah, and J. Ajienka, Review of Python applications in solving oil and gas problems. Journal of Engineering Research and Reports, 2021. 21(3): p. 13-22.

[23] Reijers, T., Stratigraphy and sedimentology of the Niger Delta. 2011.

[24] Magbagbeola, O.A. and B.J. Willis, Sequence stratigraphy and syndepositional deformation of the Agbada Formation, Robertkiri field, Niger Delta, Nigeria. AAPG bulletin, 2007. 91(7): p. 945-958.

[25] Oluwajana, O., Evaluation of hydrocarbon source rock potential of Eocene-Oligocene Akata Formation, Onshore Niger Delta Basin, Nigeria. Benin Journal of Physical Science, 2024. 1: p. 133-147.

[26] Emudianughe, J. and K. Timi-Odiase, Well Logs and Seismic Data Analysis for Hydrocarbon Prospect in Kolo Creek, Niger Delta Nigeria. FUPRE Journal of Scientific and Industrial Research, 2022. 6(1): p. p13.

[27] Ezekwe, I.C., E.O. Oshionya, and L.D. Demua, Ecological and Potential Health Effects of Hydrocarbon and Heavy Metal Concentrations in the KoloCreek Wetlands, South-South, Nigeria. International Journal of Environmental Sciences and Natural resources, 2018. 11(1): p. 001-015.

[28] Kamel, M.H. and W.M. Mabrouk, Estimating seismic impedance and elastic parameters in hydrocarbon-bearing reservoirs from acoustic logs. Journal of Petroleum Science and Engineering, 2004. 45(1-2): p. 21-29.

[29] Yilmaz, Ö., Seismic data analysis: Processing, inversion, and interpretation of seismic data. 2001: Society of exploration geophysicists.

[30] Lemaire, S., et al., On the accuracy, robustness, and performance of high order interpolation schemes for the overset method on unstructured grids. International Journal for Numerical Methods in Fluids, 2022. 94(2): p. 152-187.

[31] Davies, O.A., C. Cookey, and A.R. Amakiri, Reservoir containment characterization for carbon dioxide (CO2) geo-sequestration in the Niger delta. International Journal of Scientific Research and Engineering Development, 2021. 4(2): p. 715-724.

[32] Tiab, D. and E.C. Donaldson, Petrophysics: theory and practice of measuring reservoir rock and fluid transport properties. 2015: Gulf professional publishing.

[33] Chikezie, P.C., et al., Rock physics as a tool for seismic stratigraphy and structural interpretation of late Miocene southwestern Deep Offshore Niger Delta, West African Continental Margin. Journal of Sedimentary Environments, 2022. 7(3): p. 351-369.

[34] Morad, S., et al., The impact of diagenesis on the heterogeneity of sandstone reservoirs: A review of the role of depositional facies and sequence stratigraphy. AAPG bulletin, 2010. 94(8): p. 1267-1309.

[35] Fagbemi, O.I., et al., Focused reservoir characterization: analysis of selected sand units using well log and 3-D seismic data in'Kukih'field, Onshore Niger Delta, Nigeria. Scientific Reports, 2024. 14(1): p. 13763.

[36] Riedel, M., et al., Acoustic impedance inversion and seismic reflection continuity analysis for delineating gas hydrate resources near the Mallik research sites, Mackenzie Delta, Northwest Territories, Canada. Geophysics, 2009. 74(5): p. B125-B137.

[37] Doust, H. and E. Omatsola, Niger delta. American Association of Petroleum Geologists Memoir, 1989. 48: p. 201-238.

[38] Adagunodo, T.A., et al., Characterization of reservoirs and depositional study of JP Field, shallow offshore of Niger Delta Basin, Nigeria. Scientific African, 2022. 15: p. e01064.

[39] Ugbor, C.C., Evaluation of Hydrocarbon Reservoir in the" SIMA" Field of Niger Delta Nigeria from Interpretation of 3D Seismic and Petrophysical Log Data. International Journal of Geosciences, 2023. 14(1): p. 94-107.

[40] Bentley, M., Practical turbidite interpretation: the role of relative confinement in understanding reservoir architectures. Marine and Petroleum Geology, 2022. 135: p. 105372.

[41] Alaminiokuma, G. and C. Ugbor, Analytical velocity model for depth conversion in the subsurface facies of Agbada formation in the Niger Delta, Nigeria. The Pacific Journal of Science and Technology, 2010. 11(1): p. 563-575.

[42] Reijers, T., S. Petters, and C. Nwajide, The Niger delta basin, in Sedimentary basins of the world. 1997, Elsevier. p. 151-172.

[43] Wei, H.-H., J.-L. Liu, and Q.-R. Meng, Structural and sedimentary evolution of the southern Songliao Basin, northeast China, and implications for hydrocarbon prospectivity. AAPG bulletin, 2010. 94(4): p. 533-566.

[44] Abrams, M.A., Significance of hydrocarbon seepage relative to petroleum generation and entrapment. Marine and Petroleum Geology, 2005. 22(4): p. 457-477.